PROCEEDINGS OF SCIENCE

Comparison of the atmospheric muon flux measured by the KM3NeT detectors with the CORSIKA simulation using the Global Spline Fit model

PoS(ICRC2023)338

Andrey Romanov[a,b,*] **and Piotr Kalaczynski**[c,d] **on behalf of the KM3NeT Collaboration**

[a] *Dipartimento di Fisica dell'Università di Genova, Via Dodecaneso 33, 16146 Genova, Italy*
[b] *INFN - Sezione di Genova, Via Dodecaneso 33, 16146 Genova, Italy*
[c] *National Centre for Nuclear Research, 02-093 Warsaw, Poland*
[d] *Nicolaus Copernicus Astronomical Center Polish Academy of Sciences, Particle Astrophysics Science and Technology Centre, Rektorska 4, Warsaw, 00-614 Poland*

E-mail: aromanov@ge.infn.it, pkalaczynski@camk.edu.pl

Atmospheric muons are the dominant component of the down-going events for the KM3NeT neutrino telescopes. Deep underwater measurements of muons provide important information about the cosmic ray properties. The KM3NeT research infrastructure includes two telescopes currently in operation while still being under construction in the Mediterranean Sea. The KM3NeT/ORCA detector is deployed at 2450 m depth near Toulon, France. The KM3NeT/ARCA telescope is located at 3500 m depth off-shore Capo Passero, Italy. In this work, the measured atmospheric muon flux is compared to the Monte Carlo simulation using the CORSIKA package with the Sibyll 2.3d model for high-energy hadronic interactions and the GSF model for mass composition. The data from both KM3NeT/ORCA and KM3NeT/ARCA telescopes are considered for this analysis. In the current configuration, KM3NeT/ORCA covers cosmic ray energy range from several TeV up to hundreds of TeV per nucleon, while for KM3NeT/ARCA the range is from several TeV up to PeV per nucleon. Systematic uncertainties considered for the analysis include that on the cosmic ray flux normalization and its composition, water properties, detector response, and high-energy hadronic interaction models.

38th International Cosmic Ray Conference (ICRC2023)
26 July - 3 August, 2023
Nagoya, Japan

*Speaker

1. Introduction

The KM3NeT research infrastructure comprises two neutrino telescopes at the bottom of the Mediterranean Sea [1]. The KM3NeT/ARCA telescope is being constructed off-shore the coast of Sicily, Italy, at a depth of ~3.5 km. Its primary scientific aim is to study High-Energy (HE) cosmic neutrinos in the TeV-PeV range. The KM3NeT/ORCA detector has a smaller and denser configuration with respect to KM3NeT/ARCA since its primary goal is to investigate atmospheric neutrino oscillations and neutrino mass hierarchy which requires a lower energy threshold (GeV) for neutrino detection. The telescope is located around 40 km away from Toulon, off the coast of France, at ~2.5 km depth. An array of 115 lines is called a building block. The final configuration of the KM3NeT/ARCA telescope will comprise two building blocks and KM3NeT/ORCA will consist of one such block. The one building block configuration is called ARCA115 and ORCA115 in the following. The analysis presented in this work was performed with data taken by the KM3NeT/ARCA and KM3NeT/ORCA telescopes with six working lines each. In the following, those configurations are denoted as ARCA6 and ORCA6.

This contribution aims to compare the atmospheric muon flux measured by ARCA6 and ORCA6 detectors to the MC simulation performed with the CORSIKA package [2] that includes the Sibyll 2.3d model [3] for description of HE hadronic interactions and the Global Spline Fit (GSF) [4] as model of the mass composition of Cosmic Ray (CR) flux.

2. Simulation of atmospheric muons in KM3NeT

The simulation of atmospheric muons for the KM3NeT experiment starts in the upper layers of the atmosphere and ends deep underwater. The first step is to simulate the interactions of the primary CRs with the air nuclei and the subsequent Extensive Air Shower (EAS) development. This step is performed with the CORSIKA [2] v.7.741 package.

The minimum muon energy required to reach the top part of the KM3NeT/ORCA detector (~2 km) is around 500 GeV [5]. Hence, the lower limit on the primary energy was set to 1 TeV per nucleon in the simulation. Five nuclei were used as primaries in the simulation: proton, helium, carbon, oxygen, and iron. Other primaries were taken into account by enlarging the flux weights of C, O, and Fe according to the flux of nuclei missing in the simulation. The CR mass composition model that was used in this work is GSF [4].

The plots in Fig. 1 show the sea level flux of muon bundles that reach ORCA6 and ARCA6 detectors as a function of the bundle energy. The muon bundle energy is the sum of muon energies at sea level originating from one shower for those muons that reach the detector. The highlighted area indicates the 90% fraction of events counting from the maximum of the distribution. The energy range of the fraction spans from 0.8 TeV to 10 TeV for ORCA6 and from 1.1 TeV to 34 TeV for ARCA6. The upper limit arises due to the fast decrease of the CR flux with energy.

Therefore, the sea level energy of muons detectable by the KM3NeT experiment lays in the TeV range. This muon energy is about 3 orders of magnitude higher than for the muons detected in EAS experiments. Thus, the KM3NeT measurement is complementary to the investigations of the so-called muon puzzle [6], i.e. deficit of GeV muons detected at the ground.

PoS(ICRC2023)338

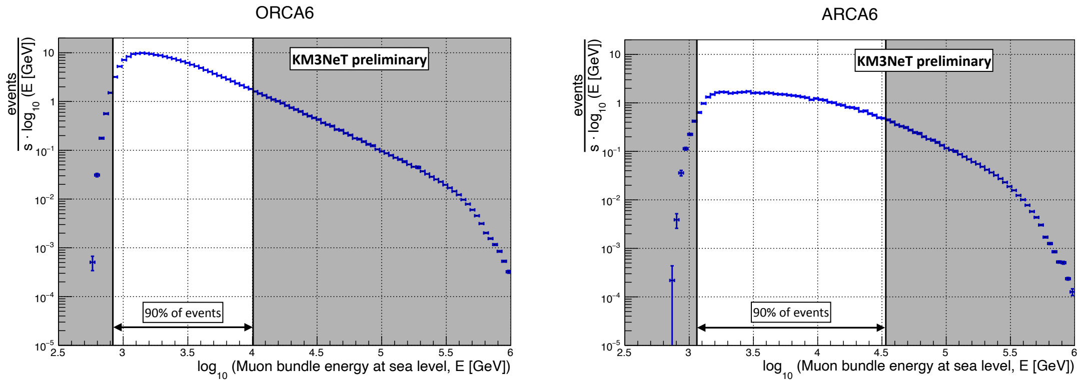

Figure 1: Sea level rate of generated muon bundles that reach the depth of the KM3NeT telescopes as a function of bundle energy. The left (right) plot shows the range for ORCA6 (ARCA6) detector.

The HE hadronic interaction model used in the simulation is Sibyll 2.3d [3]. Differences in the HE muon flux induced by choosing the different HE hadronic interaction models are treated as systematic uncertainties.

Fig. 2 shows pseudorapidity of muons reaching ORCA6 and ARCA6 detectors. The pseudorapidity is defined as $\eta = -\ln[\tan(\theta/2)]$, where θ is the angle between the primary particle and secondary muon at sea level. The peak of the distributions is located at $\eta \approx 9$. Therefore, muons seen by KM3NeT detectors originate from hadronic interactions laying in the very forward region of pseudorapidities. This region is not fully covered by accelerator experiments [6]. Hence, the hadronic interaction models that aim to describe the CR interactions that are seen by the KM3NeT detectors rely necessarily on the extrapolations of experimental results.

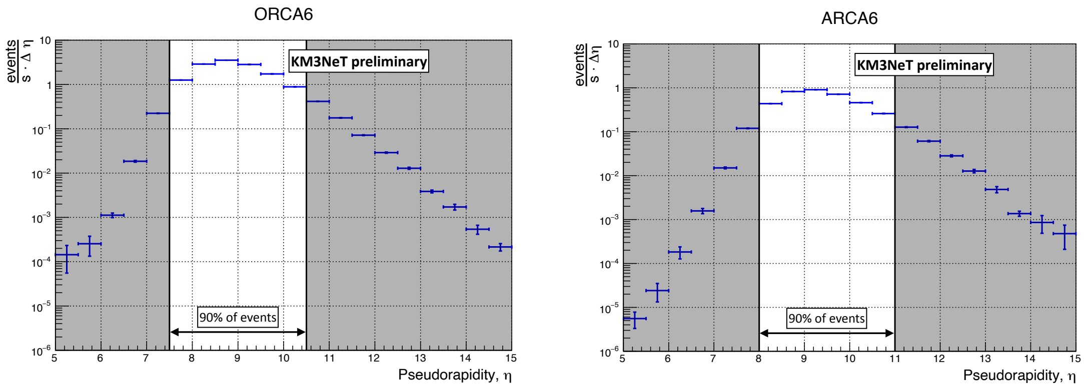

Figure 2: Pseudorapidity distribution of muons reaching ORCA6 (left plot) and ARCA6 (right plot) detectors. The highlighted area shows the energy range that includes a 90% fraction of events.

The propagation of muons in water down to the KM3NeT detectors is performed with the gSeaGen code [8] using PROPOSAL [9] as a muon propagator.

Simulation of the Cherenkov radiation induced by muons, its detection by the optical modules, and the muon track reconstruction is performed with the internal KM3NeT software.

The top part of Fig. 3 shows the rate of reconstructed events counted at ORCA6 and ARCA6 detectors as a function of the true primary nucleus energy. 90% fraction of the total number of events corresponds to the energy range from 3 to 316 TeV for ORCA6 and from 5 TeV to 1.3 PeV for ARCA6. The same distributions when considering ORCA115 and ARCA115 telescopes are presented in the bottom part of Fig. 3. The energy ranges for the these detector configurations are 3 TeV - 250 TeV for ORCA115 and 6 TeV - 1 PeV for ARCA115. For both detectors, the events mostly originate from p and He primaries.

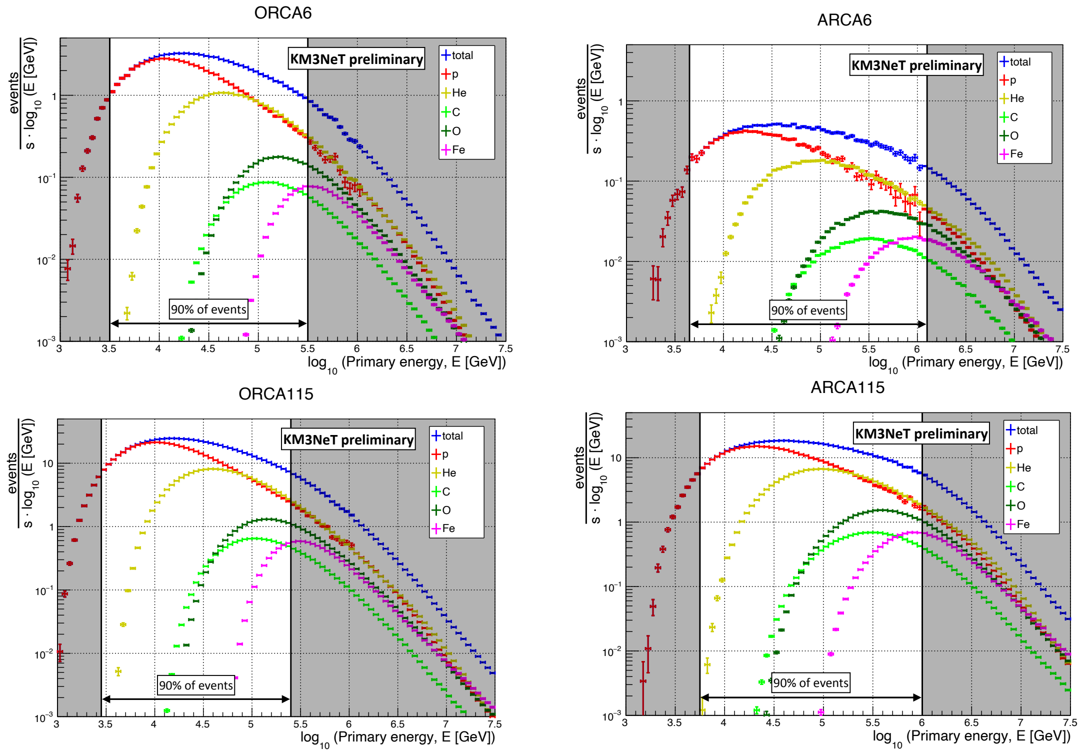

Figure 3: Rate of reconstructed atmospheric muon events expected with ORCA6 (top left plot), ARCA6 (top right plot), ORCA115 (bottom left plot), and ARCA115 (bottom right plot) detectors as a function of the primary energy. The total rate is shown in blue, the rates from p, He, C, O, and Fe primaries are shown as red, yellow, light green, dark green, and purple points, correspondingly.

3. MUPAGE tuning on CORSIKA

CORSIKA provides atmospheric muons at sea level, which can be propagated till the detector, performing the full MC simulation of EAS development through the atmosphere. The main drawback of this approach is high CPU time.

To reduce CPU time requirement, the simulation of atmospheric muons in KM3NeT is based on the fast MC generator MUPAGE [10]. It generates the muon bundle kinematics features at a certain sea depth and zenith angle based on parametric formulas. The formulas describe the flux of the single- and multi-muon bundles, the differential energy spectrum, and the lateral distance of muons from the bundle axis. Values of the parameters [11] were obtained starting from a full MC simulation performed with the HEMAS package [12] and fitting the results to MACRO [13] measurements.

With the aim of merging the advantage of a quick parameterized simulation and the details coming from the CORSIKA full simulation associated to the most recent physics models, both for hadronic interaction description (Sibyll 2.3d [3]) and for mass composition (GSF [4]), a framework was developed to adjust the MUPAGE parameters in order to reproduce CORSIKA expectations. The MUPAGE code and the parametric formulas themselves were not modified. Fig. 4 shows the muon zenith flux distributions expected with ORCA6 and ARCA6 detectors resulting from the CORSIKA full simulation and from MUPAGE with the nominal parametrization and with the modified MUPAGE tuned on CORSIKA. The distributions obtained with the *tuned* MUPAGE agree with what obtained with CORSIKA full MC within statistical fluctuations for both ORCA6 and ARCA6 detectors. Hence, the *tuned* MUPAGE can be used as a fast proxy of CORSIKA in order to obtain results that are similar to simulations with CORSIKA + Sybill 2.3d and GSF models.

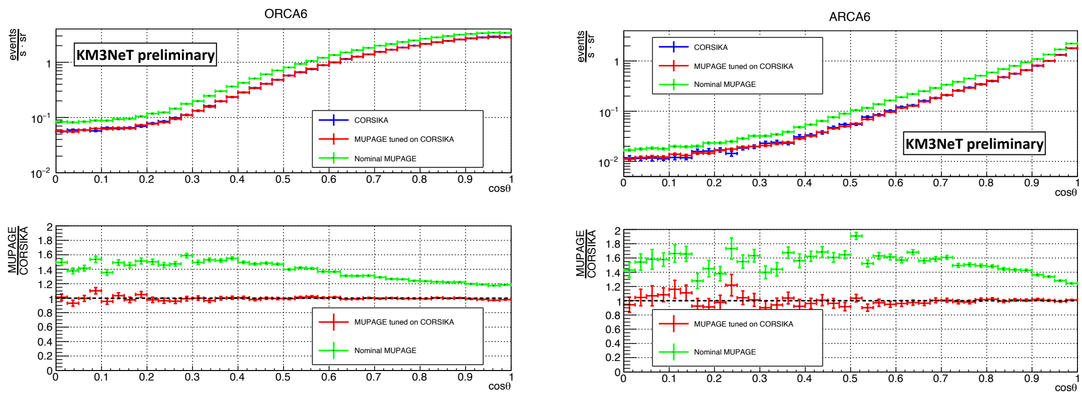

Figure 4: Rate of reconstructed atmospheric muons for ORCA6 (left plot) and ARCA6 (right plot) detectors as a function of the zenith angle. The blue (red) points represent the CORSIKA simulation. The nominal MUPAGE is shown as green points and the MUPAGE tuned on CORSIKA is shown in red. The ratios between MUPAGE and CORSIKA are on the bottom plots.

4. Reconstruction of muon arrival direction

To evaluate the direction reconstruction capabilities, the true and the reconstructed muon zenith angles, θ, were used. The true zenith angle is the one of the muon bundle at the detector can, all muons are assumed to be collinear with the bundle axis in MUPAGE. The reconstructed angle is instead obtained with the KM3NeT reconstruction algorithm. In the left plot of Fig. 5, the MC true $\cos\theta$ distribution (blue points) is compared to the reconstructed one (red points) for ORCA6 detector. The discrepancy starts to emerge for events with $\cos\theta < 0.5$. The reason for this discrepancy is that the flux dependence on $\cos\theta$ is very steep and few well-reconstructed events at $\cos\theta < 0.5$ are dominated by a fraction of mis-reconstructed vertical muons. The KM3NeT angular resolution is at sub-degree level, so the fraction of mis-reconstructed events is small, however the number of vertical muons is several orders of magnitude higher. Hence, it was decided to consider only muons with $\cos\theta > 0.5$ for the final data/MC studies. The same plot but for ARCA6 telescope is shown in the right plot of Fig. 5. Muons with $\cos\theta > 0.6$ are considered well reconstructed.

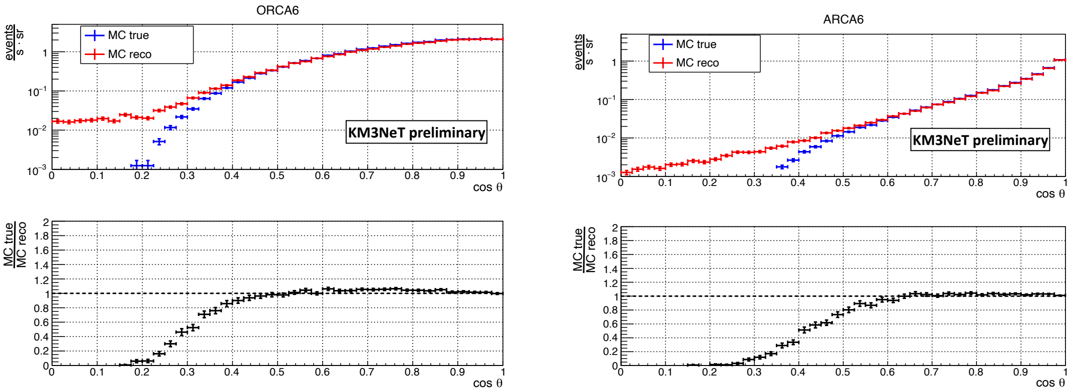

Figure 5: Distribution of the true muon bundle zenith angle at the can (blue points) compared to the reconstructed zenith angle (red points) for ORCA6 (left plot) and ARCA6 (right plot) detectors. The bottom plot shows the ratio of the distributions.

5. Data and MC with systematics

Systematic errors considered in this work include uncertainties on CR flux, light absorption length in seawater, PMT quantum efficiency, and HE hadronic interaction model.

To estimate the uncertainty on the water absorption length and PMT efficiency, ±10% variations were assumed for both quantities. The uncertainty on CR flux is evaluated using the data provided in the GSF model. The HE hadronic interaction uncertainties are estimated using the post-LHC models available in the MCEq software [14].

The final result of this analysis is the comparison of KM3NeT data with MC simulation including all systematic uncertainties mentioned above. Data and MC comparison results together with associated uncertainties are shown in Fig. 6 for ORCA6 and ARCA6 detectors. The plots below are obtained with the quality cuts on the reconstruction applied in order to remove background (^{40}K decays and bioluminescence).

The MC simulation underestimates data for both ORCA6 and ARCA6 detectors. The discrepancy for ORCA6 goes beyond the uncertainties considered in this work. The ratio between data and simulation is flat in the considered zenith angle range. There are ~40% more muons in data with respect to simulation.

The shape of the ARCA6 data/MC ratio is not flat in contrast to the ORCA6 result. One of the possible explanations for the non-flat ARCA ratio and the mismatch in the ratio values between the detectors could be related to the detector response simulation uncertainties, and in particular, water properties.

Given a discrepancy between KM3NeT data and MC simulation for the muon zenith distribution underwater, it is important to investigate if it is also present for the sea level flux of HE muons. Fig. 7 shows the sea level muon flux resulting from the CORSIKA simulation, which used for the MUPAGE tuning, compared to the real data from the ground-based experiments and to the analytical models. The x-axis range of the figure covers the 99% fraction of single muon events detected by ORCA6 and ARCA6 telescopes. The data points shown in the figure are from the experiments mentioned in the overview paper [15] and from the L3+C experiment [16]. The analytical models

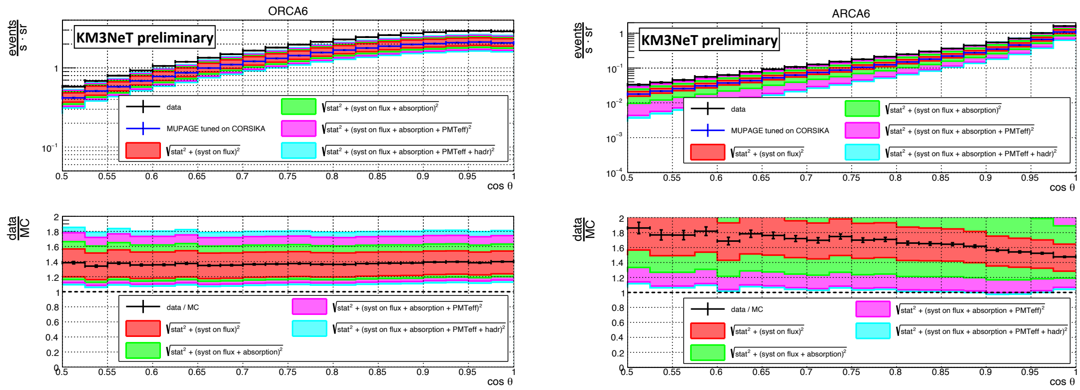

Figure 6: Comparison of the data (black points) and MC simulation results (blue points) for the atmospheric muons in terms of the zenith angle distribution for ORCA6 (left plot) and ARCA6 (right plot) detectors. The simulation includes statistical uncertainties that are shown as black vertical lines. The systematic uncertainties are shown as cumulative bands that include uncertainty on the CR flux (red band), the light absorption length (green band), the PMT efficiency (purple band), and the hadronic interaction models (light blue band).

considered are by T. Gaisser [17] and E. V. Bugaev [18]. Also, the fit of the MACRO data was added to the plot [19].

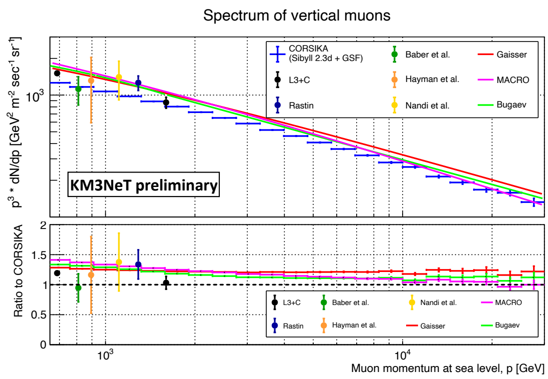

Figure 7: The sea level flux of muons from the CORSIKA simulation used in this work (blue points) compared to two analytical models, Gaisser [17] (red line) and Bugaev [18] (green line), to the fit of the MACRO data [13] (purple line), and to the experimental results from the ground-based experiments [15, 16]. The bottom plot shows the ratio of models and data to CORSIKA.

In general, CORSIKA expectations underestimate the sea level muon flux with respect to considered models. The discrepancy is at a level of 30%. All data points except for two exceed the CORSIKA predictions by ~20-30%.

The discrepancy between data and simulation for the underwater muon flux seen by ORCA6 telescope is around 40% as shown above. That indirectly confirms that the KM3NeT simulation describes the muon propagation in water, the light generation, the detector response, and the muon reconstruction with a precision better than 10%. The 10% disagreement between the simulation and measurements at sea level and underwater may be explained with uncertainties on light attenuation length in seawater and detector response simulation, shown as green and purple bands in Fig. 6.

The sum of the two aforementioned upper uncertainties is around 10% for the ORCA6 telescope and 20-40% for the ARCA6 detector that covers the difference.

The models used in this analysis include the post-LHC hadronic interaction model Sybill 2.3d and the GSF CR flux model which was fitted on the most recent direct CR measurements. The models provide a ~40% deficit in TeV muons with respect to the KM3NeT data. We hope this additional measurement provides new insights and the test-bench for possible solutions to the muon puzzle.

This contribution is supported by IRAP AstroCeNT (MAB/2018/7) funded by FNP from ERDF.

References

[1] S. Adrián Martínez et al., J. Phys. G: Nucl. Part. Phys. **43** 084001 (2016)

[2] D. Heck, J. Knapp, J. Capdevielle, G. Schatz, and T. Thouw, Report fzka 6019.11 (1998)

[3] F. Riehn, R. Engel, A. Fedynitch, T.K. Gaisser, and T. Stanev, Phys. Rev. D **102** 063002 (2020)

[4] H. P. Dembinski et al., PoS(ICRC2017)533 (2018)

[5] S. Aiello et al., Eur. Phys. J. C **83**, 344 (2023)

[6] J. Albrecht et al., Astrophys. Space Sci. **367** (2022)

[7] M. Bleicher et al., J. Phys. G **25**, 1859 (1999)

[8] S. Aiello et al., Comput. Phys. Commun. **256**, 107477 (2020)

[9] J. H. Koehne et al., Comput. Phys. Commun. **184**, 2070 (2013)

[10] G. Carminati, M. Bazzotti, A. Margiotta, and M. Spurio, Comput. Phys. Commun. **179**, 915 (2008)

[11] Y. Becherini, A.Margiotta, M. Sioli, and M. Spurio, Astropart. Phys. **25**, 1 (2006)

[12] C. Forti et al., Phys. Rev. D **42** 3668 (1990)

[13] M. Ambrosio et al., Phys. Rev. D **60** (1999) 032001

[14] A. Fedynitch, R. Engel, T. K. Gaisser, F. Riehn, and T. Stanev, EPJ Web Conf. **99**, 08001 (2015)

[15] T. Hebbeker and C. Timmermans, Astropart. Phys., 18, 107–127 (2002)

[16] P. Achard et al., Phys. Lett. B **598**, 15 (2004)

[17] Gaisser T. K., Cosmic Rays and Particle Physics, Cambridge: Cambridge Univ. Press (1990)

[18] E. Bugaev et al., Phys. Rev. D 58 054001 (1998)

[19] M. Ambrosio et al., Phys. Rev. D 52, 3793 (1995)

Full Authors List: The KM3NeT Collaboration

S. Aiello[a], A. Albert[b,bd], S. Alves Garre[c], Z. Aly[d], A. Ambrosone[f,e], F. Ameli[g], M. Andre[h], E. Androutsou[i], M. Anguita[j], L. Aphecetche[k], M. Ardid[l], S. Ardid[l], H. Atmani[m], J. Aublin[n], L. Bailly-Salins[o], Z. Bardačová[q,p], B. Baret[n], A. Bariego-Quintana[c], S. Basegmez du Pree[r], Y. Becherini[n], M. Bendahman[m,n], F. Benfenati[t,s], M. Benhassi[u,e], D. M. Benoit[v], E. Berbee[r], V. Bertin[d], S. Biagi[w], M. Boettcher[x], D. Bonanno[w], J. Boumaaza[m], M. Bouta[y], M. Bouwhuis[r], C. Bozza[z,e], R. M. Bozza[f,e], H.Brânzaş[aa], F. Bretaudeau[k], R. Bruijn[ab,r], J. Brunner[d], R. Bruno[a], E. Buis[ac,r], R. Buompane[u,e], J. Busto[d], B. Caiffi[ad], D. Calvo[c], S. Campion[g,ae], A. Capone[g,ae], F. Carenini[t,s], V. Carretero[c], T. Cartraud[n], P. Castaldi[af,s], V. Cecchini[c], S. Celli[g,ae], L. Cerisy[d], M. Chabab[ag], M. Chadolias[ah], A. Chen[ai], S. Cherubini[aj,w], T. Chiarusi[s], M. Circella[ak], R. Cocimano[w], J. A. B. Coelho[n], A. Coleiro[n], R. Coniglione[w] P. Coyle[d], A. Creusot[n], A. Cruz[al], G. Cuttone[w], R. Dallier[k], Y. Darras[ah], A. De Benedittis[e], B. De Martino[d], V. Decoene[k], R. Del Burgo[e], U. M. Di Cerbo[e], L. S. Di Mauro[w], I. Di Palma[g,ae], A. F. Díaz[j], C. Diaz[j], D. Diego-Tortosa[w], C. Distefano[w], A. Domi[ah], C. Donzaud[n], D. Dornic[d], M. Dörr[am], E. Drakopoulou[i], D. Drouhin[b,bd], R. Dvornický[q], T. Eberl[ah], E. Eckerová[q,p], A. Eddymaoui[m], T. van Eeden[r], M. Eff[n], D. van Eijk[r], I. El Bojaddaini[y], S. El Hedri[n], A. Enzenhöfer[d], G. Ferrara[w], M. D. Filipović[an], F. Filippini[t,s], D. Franciotti[w], L. A. Fusco[z,e], J. Gabriel[ao], S. Gagliardini[g], T. Gal[ah], J. García Méndez[l], A. Garcia Soto[c], C. Gatius Oliver[r], N. Geißelbrecht[ah], H. Ghaddari[y], L. Gialanella[e,u], B. K. Gibson[v], E. Giorgio[w], I. Goos[n], D. Goupilliere[o], S. R. Gozzini[c], R. Gracia[ah], K. Graf[ah], C. Guidi[ap,ad], B. Guillon[o], M. Gutiérrez[aq], H. van Haren[ar], A. Heijboer[r], A. Hekalo[am], L. Hennig[ah], J. J. Hernández-Rey[c], F. Huang[d], W. Idrissi Ibnsalih[e], G. Illuminati[s], C. W. James[al], M. de Jong[as,r], P. de Jong[ab,r], B. J. Jung[r], P. Kalaczyński[at,be], O. Kalekin[ah], U. F. Katz[ah], N. R. Khan Chowdhury[c], A. Khatun[q], G. Kistauri[av,au], C. Kopper[ah], A. Kouchner[aw,n], V. Kulikovskiy[ad], R. Kvatadze[av], M. Labalme[o], R. Lahmann[ah], G. Larosa[w], C. Lastoria[d], A. Lazo[c], S. Le Stum[d], G. Lehaut[o], E. Leonora[a], N. Lessing[c], G. Levi[t,s], M. Lindsey Clark[n], F. Longhitano[a], J. Majumdar[r], L. Malerba[ad], F. Mamedov[p], J. Mańczak[c], A. Manfreda[e], M. Marconi[ap,ad], A. Margiotta[t,s], A. Marinelli[e,f], C. Markou[i], L. Martin[k], J. A. Martínez-Mora[l], F. Marzaioli[u,e], M. Mastrodicasa[ae,g], S. Mastroianni[e], S. Micciché[w], G. Miele[f,e], P. Migliozzi[e], E. Migneco[w], M. L. Mitsou[e], C. M. Mollo[e], L. Morales-Gallegos[u,e], C. Morley-Wong[al], A. Moussa[y], I. Mozun Mateo[ay,ax], R. Muller[r], M. R. Musone[e,u], M. Musumeci[w], L. Nauta[r], S. Navas[aq], A. Nayerhoda[ak], C. A. Nicolau[g], B. Nkosi[ai], B. Ó Fearraigh[ab,r], V. Oliviero[f,e], A. Orlando[w], E. Oukacha[n], D. Paesani[w], J. Palacios González[c], G. Papalashvili[au], V. Parisi[ap,ad], E.J. Pastor Gomez[c], A. M. Păun[aa], G. E. Păvălaş[aa], S. Peña Martínez[n], M. Perrin-Terrin[d], J. Perronnel[o], V. Pestel[ay], R. Pestes[n], P. Piattelli[w], C. Poirè[z,e], V. Popa[aa], T. Pradier[b], S. Pulvirenti[w], G. Quéméner[o], C. Quiroz[l], U. Rahaman[c], N. Randazzo[a], R. Randriatoamanana[k], S. Razzaque[az], I. C. Rea[e], D. Real[c], S. Reck[ah], G. Riccobene[w], J. Robinson[x], A. Romanov[ap,ad], A. Šaina[c], F. Salesa Greus[c], D. F. E. Samtleben[as,r], A. Sánchez Losa[c,ak], S. Sanfilippo[w], M. Sanguineti[ap,ad], C. Santonastaso[ba,e], D. Santonocito[w], P. Sapienza[w], J. Schnabel[ah], J. Schumann[ah], H. M. Schutte[x], J. Seneca[r], N. Sennan[y], B. Setter[ah], I. Sgura[ak], R. Shanidze[au], Y. Shitov[p], F. Šimkovic[q], A. Simonelli[e], A. Sinopoulou[a], M.V. Smirnov[ah], B. Spisso[e], M. Spurio[t,s], D. Stavropoulos[i], I. Štekl[p], M. Taiuti[ap,ad], Y. Tayalati[m], H. Tedjditi[ad], H. Thiersen[x], I. Tosta e Melo[a,aj], B. Trocmé[n], V. Tsourapis[i], E. Tzamariudaki[i], A. Vacheret[o], V. Valsecchi[w], V. Van Elewyck[aw,n], G. Vannoye[d], G. Vasileiadis[bb], F. Vazquez de Sola[r], C. Verilhac[n], A. Veutro[g,ae], S. Viola[w], D. Vivolo[u,e], J. Wilms[bc], E. de Wolf[ab,r], H. Yepes-Ramirez[l], G. Zarpapis[i], S. Zavatarelli[ad], A. Zegarelli[g,ae], D. Zito[w], J. D. Zornoza[c], J. Zúñiga[c], and N. Zywucka[x].

[a]INFN, Sezione di Catania, Via Santa Sofia 64, Catania, 95123 Italy

[b]Université de Strasbourg, CNRS, IPHC UMR 7178, F-67000 Strasbourg, France

[c]IFIC - Instituto de Física Corpuscular (CSIC - Universitat de València), c/Catedrático José Beltrán, 2, 46980 Paterna, Valencia, Spain

[d]Aix Marseille Univ, CNRS/IN2P3, CPPM, Marseille, France

[e]INFN, Sezione di Napoli, Complesso Universitario di Monte S. Angelo, Via Cintia ed. G, Napoli, 80126 Italy

[f]Università di Napoli "Federico II", Dip. Scienze Fisiche "E. Pancini", Complesso Universitario di Monte S. Angelo, Via Cintia ed. G, Napoli, 80126 Italy

[g]INFN, Sezione di Roma, Piazzale Aldo Moro 2, Roma, 00185 Italy

[h]Universitat Politècnica de Catalunya, Laboratori d'Aplicacions Bioacústiques, Centre Tecnològic de Vilanova i la Geltrú, Avda. Rambla Exposició, s/n, Vilanova i la Geltrú, 08800 Spain

[i]NCSR Demokritos, Institute of Nuclear and Particle Physics, Ag. Paraskevi Attikis, Athens, 15310 Greece

[j]University of Granada, Dept. of Computer Architecture and Technology/CITIC, 18071 Granada, Spain

[k]Subatech, IMT Atlantique, IN2P3-CNRS, Université de Nantes, 4 rue Alfred Kastler - La Chantrerie, Nantes, BP 20722 44307 France

[l]Universitat Politècnica de València, Instituto de Investigación para la Gestión Integrada de las Zonas Costeras, C/ Paranimf, 1, Gandia, 46730 Spain

[m]University Mohammed V in Rabat, Faculty of Sciences, 4 av. Ibn Battouta, B.P. 1014, R.P. 10000 Rabat, Morocco

[n]Université Paris Cité, CNRS, Astroparticule et Cosmologie, F-75013 Paris, France

[o]LPC CAEN, Normandie Univ, ENSICAEN, UNICAEN, CNRS/IN2P3, 6 boulevard Maréchal Juin, Caen, 14050 France

[p]Czech Technical University in Prague, Institute of Experimental and Applied Physics, Husova 240/5, Prague, 110 00 Czech Republic

[q]Comenius University in Bratislava, Department of Nuclear Physics and Biophysics, Mlynska dolina F1, Bratislava, 842 48 Slovak Republic

[r]Nikhef, National Institute for Subatomic Physics, PO Box 41882, Amsterdam, 1009 DB Netherlands

[s]INFN, Sezione di Bologna, v.le C. Berti-Pichat, 6/2, Bologna, 40127 Italy

[t]Università di Bologna, Dipartimento di Fisica e Astronomia, v.le C. Berti-Pichat, 6/2, Bologna, 40127 Italy

[u]Università degli Studi della Campania "Luigi Vanvitelli", Dipartimento di Matematica e Fisica, viale Lincoln 5, Caserta, 81100 Italy

[v]E. A. Milne Centre for Astrophysics, University of Hull, Hull, HU6 7RX, United Kingdom

PoS(ICRC2023)338

[w]INFN, Laboratori Nazionali del Sud, Via S. Sofia 62, Catania, 95123 Italy
[x]North-West University, Centre for Space Research, Private Bag X6001, Potchefstroom, 2520 South Africa
[y]University Mohammed I, Faculty of Sciences, BV Mohammed VI, B.P. 717, R.P. 60000 Oujda, Morocco
[z]Università di Salerno e INFN Gruppo Collegato di Salerno, Dipartimento di Fisica, Via Giovanni Paolo II 132, Fisciano, 84084 Italy
[aa]ISS, Atomistilor 409, Măgurele, RO-077125 Romania
[ab]University of Amsterdam, Institute of Physics/IHEF, PO Box 94216, Amsterdam, 1090 GE Netherlands
[ac]TNO, Technical Sciences, PO Box 155, Delft, 2600 AD Netherlands
[ad]INFN, Sezione di Genova, Via Dodecaneso 33, Genova, 16146 Italy
[ae]Università La Sapienza, Dipartimento di Fisica, Piazzale Aldo Moro 2, Roma, 00185 Italy
[af]Università di Bologna, Dipartimento di Ingegneria dell'Energia Elettrica e dell'Informazione "Guglielmo Marconi", Via dell'Università 50, Cesena, 47521 Italia
[ag]Cadi Ayyad University, Physics Department, Faculty of Science Semlalia, Av. My Abdellah, P.O.B. 2390, Marrakech, 40000 Morocco
[ah]Friedrich-Alexander-Universität Erlangen-Nürnberg (FAU), Erlangen Centre for Astroparticle Physics, Nikolaus-Fiebiger-Straße 2, 91058 Erlangen, Germany
[ai]University of the Witwatersrand, School of Physics, Private Bag 3, Johannesburg, Wits 2050 South Africa
[aj]Università di Catania, Dipartimento di Fisica e Astronomia "Ettore Majorana", Via Santa Sofia 64, Catania, 95123 Italy
[ak]INFN, Sezione di Bari, via Orabona, 4, Bari, 70125 Italy
[al]International Centre for Radio Astronomy Research, Curtin University, Bentley, WA 6102, Australia
[am]University Würzburg, Emil-Fischer-Straße 31, Würzburg, 97074 Germany
[an]Western Sydney University, School of Computing, Engineering and Mathematics, Locked Bag 1797, Penrith, NSW 2751 Australia
[ao]IN2P3, LPC, Campus des Cézeaux 24, avenue des Landais BP 80026, Aubière Cedex, 63171 France
[ap]Università di Genova, Via Dodecaneso 33, Genova, 16146 Italy
[aq]University of Granada, Dpto. de Física Teórica y del Cosmos & C.A.F.P.E., 18071 Granada, Spain
[ar]NIOZ (Royal Netherlands Institute for Sea Research), PO Box 59, Den Burg, Texel, 1790 AB, the Netherlands
[as]Leiden University, Leiden Institute of Physics, PO Box 9504, Leiden, 2300 RA Netherlands
[at]National Centre for Nuclear Research, 02-093 Warsaw, Poland
[au]Tbilisi State University, Department of Physics, 3, Chavchavadze Ave., Tbilisi, 0179 Georgia
[av]The University of Georgia, Institute of Physics, Kostava str. 77, Tbilisi, 0171 Georgia
[aw]Institut Universitaire de France, 1 rue Descartes, Paris, 75005 France
[ax]IN2P3, 3, Rue Michel-Ange, Paris 16, 75794 France
[ay]LPC, Campus des Cézeaux 24, avenue des Landais BP 80026, Aubière Cedex, 63171 France
[az]University of Johannesburg, Department Physics, PO Box 524, Auckland Park, 2006 South Africa
[ba]Università degli Studi della Campania "Luigi Vanvitelli", CAPACITY, Laboratorio CIRCE - Dip. Di Matematica e Fisica - Viale Carlo III di Borbone 153, San Nicola La Strada, 81020 Italy
[bb]Laboratoire Univers et Particules de Montpellier, Place Eugène Bataillon - CC 72, Montpellier Cédex 05, 34095 France
[bc]Friedrich-Alexander-Universität Erlangen-Nürnberg (FAU), Remeis Sternwarte, Sternwartstraße 7, 96049 Bamberg, Germany
[bd]Université de Haute Alsace, rue des Frères Lumière, 68093 Mulhouse Cedex, France
[be]AstroCeNT, Nicolaus Copernicus Astronomical Center, Polish Academy of Sciences, Rektorska 4, Warsaw, 00-614 Poland

Acknowledgements

The authors acknowledge the financial support of the funding agencies: Agence Nationale de la Recherche (contract ANR-15-CE31-0020), Centre National de la Recherche Scientifique (CNRS), Commission Européenne (FEDER fund and Marie Curie Program), LabEx UnivEarthS (ANR-10-LABX-0023 and ANR-18-IDEX-0001), Paris Île-de-France Region, France; Shota Rustaveli National Science Foundation of Georgia (SRNSFG, FR-22-13708), Georgia; The General Secretariat of Research and Innovation (GSRI), Greece Istituto Nazionale di Fisica Nucleare (INFN), Ministero dell'Università e della Ricerca (MIUR), PRIN 2017 program (Grant NAT-NET 2017W4HA7S) Italy; Ministry of Higher Education, Scientific Research and Innovation, Morocco, and the Arab Fund for Economic and Social Development, Kuwait; Nederlandse organisatie voor Wetenschappelijk Onderzoek (NWO), the Netherlands; The National Science Centre, Poland (2021/41/N/ST2/01177); The grant "AstroCeNT: Particle Astrophysics Science and Technology Centre", carried out within the International Research Agendas programme of the Foundation for Polish Science financed by the European Union under the European Regional Development Fund; National Authority for Scientific Research (ANCS), Romania; Grants PID2021-124591NB-C41, -C42, -C43 funded by MCIN/AEI/ 10.13039/501100011033 and, as appropriate, by "ERDF A way of making Europe", by the "European Union" or by the "European Union NextGenerationEU/PRTR", Programa de Planes Complementarios I+D+I (refs. ASFAE/2022/023, ASFAE/2022/014), Programa Prometeo (PROMETEO/2020/019) and GenT (refs. CIDEGENT/2018/034, /2019/043, /2020/049. /2021/23) of the Generalitat Valenciana, Junta de Andalucía (ref. SOMM17/6104/UGR, P18-FR-5057), EU: MSC program (ref. 101025085), Programa María Zambrano (Spanish Ministry of Universities, funded by the European Union, NextGenerationEU), Spain; The European Union's Horizon 2020 Research and Innovation Programme (ChETEC-INFRA - Project no. 101008324).